2D MODELING OF PULSED THZ INTERROGATION OF SOFI WITH KNIT LINES

H. T. Banks[1], N. L. Gibson[1], and W. P. Winfree[2]

[1]Center for Research and Scientific Computation, Box 8205, North Carolina State University, Raleigh, NC 27606-8205
[2]NASA Langley Research Center, MS 231, Hampton, VA 23681-2199

ABSTRACT. This paper examines the scattering effect of knit lines and voids in SOFI through simulations of THz interrogation at non-normal angles of incidence using focused single-cycle plane waves. We model the electromagnetic field using the TE mode of the 2D Maxwell's equations reduced to a wave equation, which are then solved with a finite-element time-domain method. The knit lines are modeled by changing the dielectric constant.

Keywords: THz interrogation, SOFI, knit lines, FEM, time domain.
PACS: 41.20.Jb, 02.60.Cb, 02.70.Dh

INTRODUCTION

Pulsed THz frequency waves have been shown to be particularly useful for the detection of voids in the Sprayed on Foam Insulation (SOFI) used on the Space Shuttle's Thermal Protection System (TPS) [1]. However, the modeling of the propagation of a THz pulse inside of a material which exhibits heterogeneous micro-structures of sizes that are on the order of the wave length of the interrogating field is not straight-forward. Additionally, data on the dielectric properties of low density foam in the THz regime is rather sparse. Initial efforts to remedy this deficiency can be found in [2].

As discussed in [3], usual approaches to THz interrogation of SOFI generally employ signal processing techniques (for example, see [4]), which do not take advantage of much of the information contained in the reflected data signal. A physics based model may be able to more accurately describe defects [5].

Previous efforts [5,6] investigated the application of polarization mechanisms to account for the attenuation of wave propagation in foam, but matching the simulations to experimental data has yet to be completely successful. While these models were expressed in only one spatial dimension, the 2D formulation in [3] allowed for non-normally incident

CP894, *Review of Quantitative Nondestructive Evaluation Vol. 26,* ed. by D. O. Thompson and D. E. Chimenti

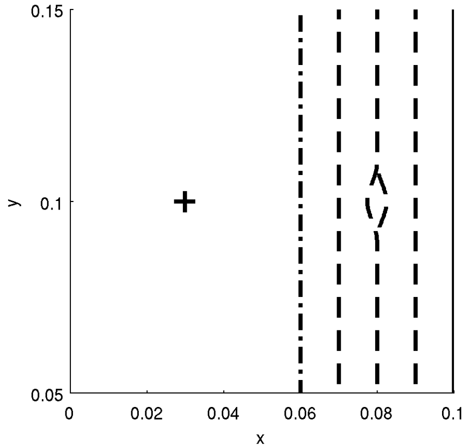

FIGURE 1: Schematic of a plane wave approaching a domain containing knit lines and an elliptical void. Dashed lines represent knit lines, dot-dash is foam/air interface. Elliptical pocket (5 mm wide) between knit lines is a void modeled by $n = 1$. "+" marks the signal receiver. Back wall is perfect conductor.

angles and curved interfaces. Further, by allowing the dielectric constant to be piecewise-constant, layers of differing densities can be modeled explicitly.

SOFI is applied in layers, producing interfaces between layers that have increased density (called "knit lines") which scatter the interrogating waveform. As the knit lines are generally on the order of $.5$ mm thick, they are frequently ignored in simulations. But the aggregate effect on the interrogating signal can be significant. This paper describes our efforts to understand and quantify the scattering mechanisms, as well as to minimize their effects by the use of focusing and/or altering the angle of incidence. We consider the scattering of a THz plane wave off of the knit lines, modeled as layers of increased density, and voids, modeled as pockets of no density, inside a block of low density polyurethane foam.

An outline of the paper is as follows. First we present the particular form of Maxwell's equations we use to model the 2D electromagnetic interrogation problem for foam. Then an experimentally based approach for estimating the material parameters for use in the system is described. We next briefly report on our numerical techniques for solving the resulting system. Finally we present simulations for cases in which the angle of incidence is altered, and the plane wave is focused to a point.

A SIMPLIFIED MATHEMATICAL MODEL

For the computational domain we take a rectangular region $0 \leq x \leq 0.1$ m and $0 \leq y \leq 0.2$ m. Figure 1 shows a schematic region containing a material with knit lines (represented by dashed lines) 1mm from each other, each parallel to an approaching plane wave, and perpendicular to the direction of propagation. The regions between knit lines consist of a low density material, and the elliptical pocket (void) is modeled as having zero density. The far right boundary ($x = 0.1$) is assumed to be metallic. A vacuum is present to the left of the material in which the interrogating field will be generated.

We combine the TE mode of the two dimensional Maxwell's equations into one equation

$$\epsilon(\vec{x})\frac{\partial^2 E}{\partial t}(t,\vec{x}) + \nabla \cdot \left(\frac{1}{\mu(\vec{x})}\nabla E(t,\vec{x})\right) = -\frac{\partial J_s}{\partial t}(t,\vec{x}), \tag{1}$$

where $\epsilon(\vec{x})$ and $\mu(\vec{x})$ are the spatially dependent dielectric permittivity and permeability, respectively. The corresponding speed of propagation is

$$c(\vec{x}) = \frac{c_0}{n(\vec{x})} = \sqrt{\frac{1}{\epsilon(\vec{x})\mu(\vec{x})}},$$

where c_0 is the speed in a vacuum.

For our source current, J_s, we want to simulate a windowed THz pulse, in this case a signal that is allowed to oscillate for one half of one period and then is truncated. For a plane wave source, see [7]. As generators actually produce a curved, sometimes spherical wave, we use a scattered field formulation to reflect the plane wave off an elliptical conductor focused at a point in the material.

To model a metallic backing behind the foam, we use reflecting (Dirichlet) boundary conditions

$$[E]_{x=0.1} = 0.$$

In order to have a finite computational domain, we impose first order absorbing boundary conditions on each of the other boundaries. For example, at $x = 0$, the condition is modeled as

$$\left.\frac{\partial E}{\partial t} - c(\vec{x})\frac{\partial E}{\partial x}\right|_{x=0} = 0.$$

Finally, we also assume zero initial conditions for E and $\dot{E}$.

The speed of propagation in the domain is given by

$$c(\vec{x}) = \frac{c_0}{n(\vec{x})} = \sqrt{\frac{1}{\epsilon(\vec{x})\mu_0}},$$

where c_0 is the speed in a vacuum and n is the index of refraction. We model knit lines by changing the index of refraction, thus effectively the speed, in that region.

In order to model the speed of wave propagation in the knit lines versus the material surrounding them, we need to be able to distinguish between the respective indices of refraction, i.e., n_1 in the low density region, and n_2 in the higher density knit line. Further, we can currently only measure the effective index of refraction of the composite material, n_e, which is done by computing the "time of flight" in experiments. Experiments have suggested, via time-of-flight measurements, a value for the effective index of refraction as $n_e = 1.03225 \pm 0.001$. To estimate the index of refraction for foam in the absence of knit lines, blocks of $5cm \times 5cm$ blocks of foam with varying numbers of knit lines layers (between 3 and 7, approximated to the nearest .25) were produced and interrogated. By calculating the velocity of the pulse in these blocks we may extrapolate the data to the case of zero knit line layers. Figure 2 displays the data collected in the experiment.

A line of best fit, computed using linear regression, is plotted in Figure 2 with error bars of two standard deviations. The range of values corresponding to zero knit lines is the estimate for the velocity of the pulse in a region of foam without knit lines. The mean value in this region is $2.94638 \times 10^8 m/s$ resulting in an index of refraction for the low density region of $n_1 = 1.0172$. Using $n_e = (1-\nu)n_1 + \nu n_2$, where ν is the volume fraction of the knit line region in the foam block. This gives the index in the knit line as $n_2 = 1.1869$.

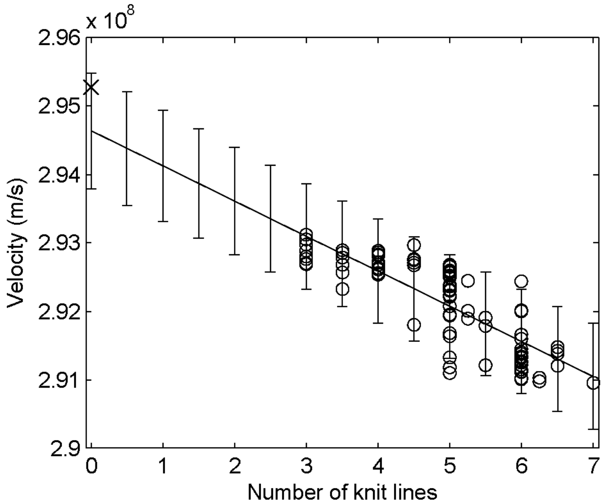

FIGURE 2: Experimental data for the velocity of a THz pulse versus the number of knit lines, with the line of best fit from applying linear regression. The error bars represent two standard deviations; the "X" denotes the Claussius-Mossotti estimate (see [7]).

NUMERICAL METHOD

We employ a (second order) Finite Element method using standard linear two dimensional ($Q1$) basis elements to spatially discretize the model described by (1). This results in nine-banded mass and stiffness matrices, M and S. We also have a contribution from absorbing boundaries which we denote with B. Thus our semi-discrete system for the vector of electric field values e is

$$M\ddot{e} + B\dot{e} + Se = f.$$

Here we have absorbed coefficients $\frac{1}{c^2}$ and $\frac{1}{c}$ into the definitions of M and B, respectively.

For the time derivatives we use second order discretizations (centered differences) for both the first and second derivatives. After collecting all terms involving the updated time step into the left hand side of the equation we have the following linear system

$$Ae_{n+1} = b, \tag{2}$$

where A contains multiples of M and B, and b depends on e_n and e_{n-1}, as well as S and f.

As discussed in [3], a mass-lumping approach, using a quadrature rule applied to the basis functions, is most efficient for solving the linear system (2) on each time step considering the length of time span required for propagation problems of this type. LU factorization is limited by memory constraints for large problems, and iterative methods are restricted by computational time.

SIMULATIONS

We compute numerical simulations of an electromagnetic wave propagating through a material described by its index of refraction, which determines the speed of propagation.

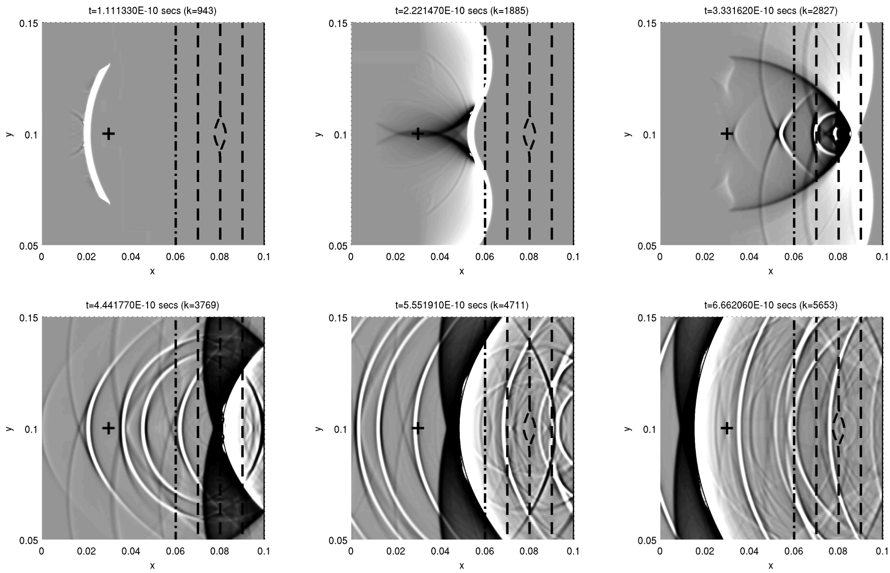

FIGURE 3: Surface plots of solutions for the case where the focused wave pulse is normally incident on the material.

We consider the presence of a void similar to what is seen in SOFI when a layer does not completely fill a recess formed in the previous layer. The void is modeled by taking its index of refraction to be that of free space, i.e., $n_0 = 1$. The knit lines are modeled with index of refraction, n_2, and the surrounding low density regions are described by n_1.

Figure 3 displays snapshots in time of the simulated propagation of a focused wave normally incident on a void in the material. The cross denotes the location of the receiver to collect data. The reflection from the void is clearly seen in the third frame. This reflection expands out to form an oblong elliptical wave which eventually returns to the antenna where the signal is recorded with a receiver. Figure 4 displays snapshots of the simulated propagation of a focused wave incident at an oblique angle on a void in the material. The cross again denotes the location of the receiver to collect data; it has been raised in the y direction to collect the center of the focused wave reflection.

The plots in Figure 5 give the simulated data collected at the receiver for the focused wave incident at normal (Figure 3) and non-normal (Figure 4) angles, respectively. In the plot the relative magnitude of the reflection versus the interrogating signal is apparent. The inset displays a magnified plot of the reflection from the void. There is a distinct difference in the structure of the two reflections. In particular, the front part of the void reflection is clearly more pronounced in the normally incident case. This suggests that simulations which do not take the proper angle of incidence into account may grossly over-exaggerate the magnitude of the reflection from the void. Also, as demonstrated in [7], the focused wave returns a larger amplitude reflection from the void. It is important that any model of a focused pulse validate basic principles such as this.

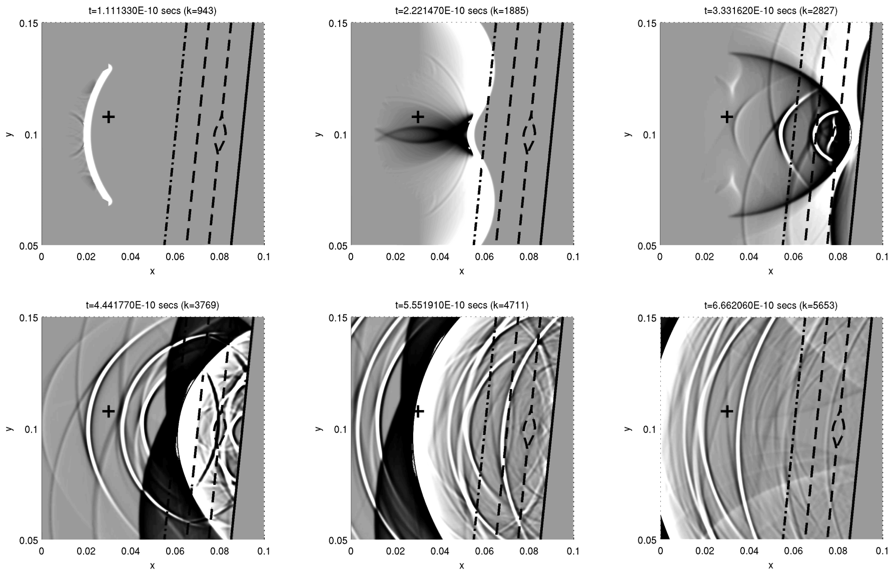

FIGURE 4: Surface plots of solutions for the case where the focused wave pulse is non-normally incident on the material.

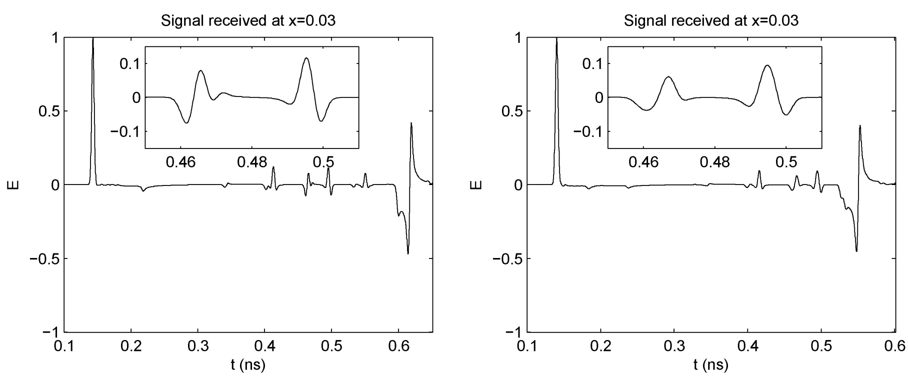

FIGURE 5: The left (right) plot displays the signal received at $x = 0$ on center line for the normally (non-normally) incident focused wave. The inset plot is a magnification of the reflection from the void.

CONCLUSIONS

We have developed a framework which accounts for the presence of knit lines in modeling the electromagnetic propagation of interrogating pulses in SOFI. We were able to compute, using results from a laboratory experiment, estimates for the index of refraction in both the knit lines and the surrounding low-density foam based on measured values from time-of-flight experiments and observable material properties.

Our efforts here provide an approach to enhance the accuracy of a model by making it more representative of the material in question and the signal used to interrogate that material. The results themselves suggest that accurate modeling of the angle of incidence is important to quantify the amplitude of the reflected signal, while modeling the focusing captures the clear distinction between the reflections from the front versus the back of the void.

Sufficient experimental results for comparison are difficult to obtain since the amplitude of reflections off of low density materials is very low to immeasurable using currently available power sources at the THz frequency. Therefore, the results of this paper should be considered as motivation for the development of high power THz devices. For now, experimental information is collected from the aluminum reflection. More work needs to be done to match simulations to this data, including adding attenuation, possibly via coupling Maxwell's equations to a time domain model of a scattering mechanism.

ACKNOWLEDGEMENTS

This research was supported in part by the U.S. Air Force Office of Scientific Research under grant AFOSR FA9550-04-1-0220 and in part by the National Institute of Aerospace (NIA) and NASA under grant NIA/NCSU-03-01-2536-NC.

REFERENCES

1. J. Xu, et. al., CLEO 2004, San Francisco, CA, May 2004.
2. G. Zhao, M. Mors, T. Wenckebach, and P. Planken, J. Opt. Soc. Amer. B, vol. 19, pp. 1476-1476, 2002.
3. H. T. Banks and N. L. Gibson, Tech. Rep. CRSC-TR06-05, NCSU, 2006. To appear in Mathematical and Computer Modelling.
4. H. Zhong, J. Xu, X. Xie, T. Yuan, R. Reightler, E. Madaras, and X.-C. Zhang, IEEE Sensors Journal, vol. 5, **2**, pp. 203-208, 2005.
5. H. T. Banks, N. L. Gibson and W. P. Winfree, *Nonlinear Analysis: Real World Applications* **6**, 381-416, 2005. Tech. Rep. CRSC-TR03-40, NCSU, 2003.
6. H. T. Banks and N. L. Gibson, Tech. Rep. CRSC-TR05-29, NCSU, 2005. To appear in the Quarterly of Applied Mathematics.
7. H. T. Banks, N. L. Gibson and W. P. Winfree, Tech. Rep. CRSC-TR06-22, NCSU, 2006.